4-11-2023

"Helicase" activity promoted through dynamic interactions between a ssDNA translocase and a diffusing SSB protein

Kacey N Mersch

Joshua E Sokoloski

Binh Nguyen

Roberto Galletto

Timothy M Lohman

PNAS RESEARCH ARTICLE | BIOCHEMISTRY

"Helicase" activity promoted through dynamic interactions between a ssDNA translocase and a diffusing SSB protein

Kacey N. Mersch[a,1], Joshua E. Sokoloski[a,b,1], Binh Nguyen[a], Roberto Galletto[a,2], and Timothy M. Lohman[a,2]

Edited by Peter von Hippel, University of Oregon, Eugene, OR; received September 30, 2022; accepted March 6, 2023

Replication protein A (RPA) is a eukaryotic single-stranded (ss) DNA-binding (SSB) protein that is essential for all aspects of genome maintenance. RPA binds ssDNA with high affinity but can also diffuse along ssDNA. By itself, RPA is capable of transiently disrupting short regions of duplex DNA by diffusing from a ssDNA that flanks the duplex DNA. Using single-molecule total internal reflection fluorescence and optical trapping combined with fluorescence approaches, we show that *S. cerevisiae* Pif1 can use its ATP-dependent 5′ to 3′ translocase activity to chemomechanically push a single human RPA (hRPA) heterotrimer directionally along ssDNA at rates comparable to those of Pif1 translocation alone. We further show that using its translocation activity, Pif1 can push hRPA from a ssDNA loading site into a duplex DNA causing stable disruption of at least 9 bp of duplex DNA. These results highlight the dynamic nature of hRPA enabling it to be readily reorganized even when bound tightly to ssDNA and demonstrate a mechanism by which directional DNA unwinding can be achieved through the combined action of a ssDNA translocase that pushes an SSB protein. These results highlight the two basic requirements for any processive DNA helicase: transient DNA base pair melting (supplied by hRPA) and ATP-dependent directional ssDNA translocation (supplied by Pif1) and that these functions can be unlinked by using two separate proteins.

RPA | DNA motors | single-molecule fluorescence | optical tweezers | dynamics

Significance

RPA is a single-stranded (ss) DNA-binding protein (SSB) in eukaryotes that binds to ssDNA formed transiently during genome maintenance and disrupts DNA secondary structures within ssDNA. We show that Pif1, a ssDNA translocase, can chemomechanically push human RPA along ssDNA and into duplex DNA, resulting in directional unwinding of duplex DNA. The results demonstrate a mechanism in which RPA gains the ability to unwind DNA directionally, an activity heretofore ascribed only to helicases. These results further show that the two basic functions of a processive helicase can be "unlinked" and provided by separate proteins, one carrying the DNA base pair melting activity and the other carrying the (ATPase-driven) translocase activity. This introduces opportunities to better understand helicase mechanisms.

Single-stranded (ss) DNA-binding (SSB) proteins are essential for all aspects of genome maintenance. They function by binding to ssDNA formed transiently during DNA replication, recombination, and repair to protect the strands from chemical and enzymatic attack, to disrupt the formation of secondary structure in the unpaired ssDNA, and to recruit other proteins and enzymes to their sites of action. In eukaryotes, the primary SSB is replication protein A (RPA), a heterotrimer with multiple oligosaccharide/oligonucleotide binding (OB) fold domains. Human (h) RPA consists of a 70 kDa Rpa1 subunit containing 4 OB folds (F, A, B, and C), a 32 kDa Rpa2 subunit with 1 OB fold (D), and a 14 kDa Rpa3 subunit with 1 OB fold (E) (1, 2). Although hRPA binds ssDNA with quite high affinity, its DNA binding is dynamic (1, 3, 4). hRPA can diffuse along ssDNA, and this diffusion is central to the mechanism by which hRPA can transiently disrupt DNA secondary structure (hairpins) that it encounters along the ssDNA (3, 5), similar to the activity observed for *E. coli* SSB protein (6, 7).

During DNA replication, recombination, and repair, SSB–ssDNA complexes form transiently since their displacement or transfer from ssDNA must occur before dsDNA can be reformed. Such reorganization of SSB–ssDNA complexes can occur by mechanisms such as complex dissociation or direct transfer to another segment of ssDNA (8, 9) or through active SSB exchange (10, 11). We demonstrated that superfamily (SF) 1 ssDNA translocases are able to chemomechanically push *E. coli* SSB tetramers along ssDNA using their ATP-dependent directional motor activity (12). It has also been shown that ssDNA translocases can displace RPA from ssDNA (13).

Using two complementary single-molecule approaches (smTIRF microscopy and dual optical-trapping combined with fluorescence confocal microscopy), we report that hRPA can be pushed along ssDNA by the chemomechanical action of the *Sc*Pif1 ssDNA translocase in the same manner as *E. coli* SSB tetramers (12), even though these two SSBs are structurally very different (14). We further show that under conditions in which ScPif1 does not act as a helicase, it can use its ssDNA translocase activity to push hRPA directionally into duplex DNA, resulting in a long-lived disruption beyond the limits that hRPA could achieve by simple diffusion (3). Hence, the actions of a diffusing SSB protein and a directional ssDNA translocase motor can be combined to generate a "helicase" activity that may function to generate ssDNA flanking regions that can be used to initiate DNA repair processes or to regulate access to the 3′ end of a ss/dsDNA junction. These

Author contributions: K.N.M., J.E.S., R.G., and T.M.L. designed research; K.N.M. and J.E.S. performed research; K.N.M., J.E.S., B.N., R.G., and T.M.L. contributed new reagents/analytic tools; K.N.M., J.E.S., R.G., and T.M.L. analyzed data; and K.N.M., J.E.S., R.G., and T.M.L. wrote the paper.

The authors declare no competing interest.

This article is a PNAS Direct Submission.

[1]K.N.M. and J.E.S. contributed equally to this work.

[2]To whom correspondence may be addressed. Email: galletto@wustl.edu or lohman@wustl.edu.

This article contains supporting information online at https://www.pnas.org/lookup/suppl/doi:10.1073/pnas.2216777120/-/DCSupplemental.

Published April 3, 2023.

results also bear on the mechanistic requirements needed for any processive helicase and that the two basic functions can be provided by separate proteins, one carrying the DNA base pair melting activity and the other carrying the (ATPase-driven) translocase activity. The demonstration that these basic functions can be "unlinked" introduces opportunities to more clearly understand the mechanisms of "standard" helicases.

Results

Replication Protein A Diffuses along ssDNA. Using a single-molecule total internal reflection fluorescence (smTIRF) microscopy assay, Nguyen et al. (3) showed that hRPA can diffuse along ssDNA. A one-dimensional diffusion coefficient on ssDNA of ~3,000 nt^2/s was estimated for human RPA (hRPA) at 25 °C (500 mM NaCl) based on modeling of the smTIRF data. Here, we used a smTIRF FRET assay to demonstrate hRPA diffusion along a short 60-nucleotide ssDNA as described (3). In this case, ssDNA labeled with a Cy3 fluorophore at its 3′ end (3′-dT-Cy3-$(dT)_{60}$) was hybridized to a biotinylated 18-bp dsDNA handle and immobilized on the surface of a neutravidin-treated biotinylated-PEG-coated coverslip (Fig. 1*A*). The sequence and structures of all smTIRF DNA substrates are given in *SI Appendix*, Table S1 and S2. smTIRF measurements were performed in buffer A at 25 °C (*Materials and Methods*). Stable Cy3 emission was observed while imaging DNA alone (Fig. 1*A*). When Cy5-labeled human RPA (Cy5-hRPA) (*Materials and Methods*) (100 pM to 1 nM) was added to the immobilized DNA, followed by washing out unbound hRPA, the formation of Cy5-hRPA/DNA complexes resulted in the appearance of fluctuating anticorrelated Cy3 and Cy5 fluorescence changes (Fig. 1*B*). The fluctuating FRET signal results from the random diffusion of hRPA along the ssDNA such that the Cy5-hRPA transiently approaches and recedes from the Cy3 at the 3′ end of the DNA (3).

In order to analyze hRPA diffusion along ssDNA quantitatively and obtain an estimate of a one-dimensional diffusion coefficient, we used confocal scanning microscopy paired with optical tweezers (LUMICKS C-Trap G2). In these experiments, the ends of a long (20,452 nt) ssDNA were held under tension between two optical traps in a Lumicks flow cell. The ssDNA tether was formed by capturing the ends between two streptavidin-coated polystyrene beads of the 20,452-bp dsDNA construct containing a 5x-biotin tag on both the 3′ and 5′ end of one strand of the DNA duplex (*SI Appendix*, Fig. S1*A*). Increasing tension was applied to the dsDNA tether up to ~82 pN and held momentarily at this force to allow the strand lacking the biotin tags to dissociate from the tethered DNA strand (*SI Appendix*, Fig. S1*B*). A force-extension profile was obtained, confirming that the tethered DNA was ssDNA.

Following generation of a ssDNA tether and binding of Cy5-hRPA (*SI Appendix*, Fig. S1*A*), the movement of Cy5-hRPA along the ssDNA was monitored by holding the ssDNA tether under tension while scanning the length of the ssDNA in 27.2-ms increments using a 638-nm confocal laser. Fig. 2*A* shows a kymograph monitoring four Cy5-hRPA molecules bound to the ssDNA under 10 pN of force, imaged at 30 °C in buffer B (pH 8.1, 100 mM NaCl). We obtained trajectories for 159 Cy5-hRPA molecules, and these are all displayed in Fig. 2*B*, with the initial position of each trace offset to start at zero. These data show that the Cy5-hRPA trajectories adhere to simple diffusional behavior, as the traces in Fig. 2*B* exhibit dynamic movements away from an initial starting point. Furthermore, the mean displacement of Cy5-hRPA molecules (orange line) follows closely along the zero position, indicating that, on average, the molecules exhibit no net displacement on ssDNA, consistent with simple Brownian diffusion.

We obtained quantitative estimates of one-dimensional diffusion coefficients (D_1) for Cy5-hRPA on ssDNA held at three forces (10, 7.5, and 5 pN). Plots of the mean squared displacement (MSD) as a function of time at each force are shown in *SI Appendix*, Fig. S2, with the MSD for each trajectory calculated using Eq. **1** (*Materials and Methods*). The data at each force were fit by linear regression and diffusion coefficients obtained from the slopes divided by two, since MSD = 2Dt. The resulting mean diffusion coefficient estimates (Table 1) show little dependence on force, with an average mean one-dimensional diffusion coefficient, D_1 = 2,806 ± 153 nt^2/s at 30 °C (100 mM NaCl). We observe only a slight effect of force on hRPA dissociation from the ssDNA (*SI Appendix*, Fig. S2). This contrasts with results for *E. coli* SSB tetramer diffusion on ssDNA that show significantly increased rates of dissociation at forces in the ~10 to 12 pN range (15).

We also examined the effect of [NaCl] on D_1 (65 mM, 100 mM, 250 mM, and 500 mM NaCl) at 30 °C in buffer B. Fig. 2*C*

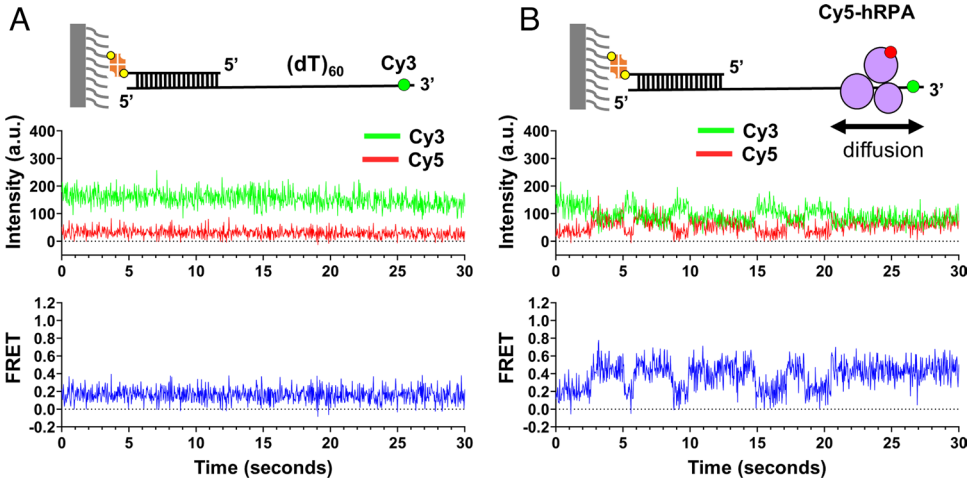

Fig. 1. hRPA diffuses along single-stranded DNA. (*A*) Representative time trajectory from a smTIRF experiment for a single molecule of 3′-Cy3-labeled $(dT)_{60}$ ssDNA immobilized on the surface of a coverslip as shown in the cartoon. Analysis of 1,047 trajectories yielded 1,012 that exhibit stable Cy3 emission as shown in panel (*A*) and 35 trajectories exhibiting photobleaching or blinking. (*B*) To monitor protein diffusion, a single Cy5-hRPA was bound to the surface immobilized Cy3-labeled ssDNA substrate as depicted in the cartoon. The anticorrelated Cy3 and Cy5 time trajectories and the resulting FRET fluctuations reflect the diffusion of Cy5-hRPA along ssDNA. Analysis of 1,055 trajectories yielded 141 exhibiting dynamic anticorrelated behavior as shown in panel (*B*).

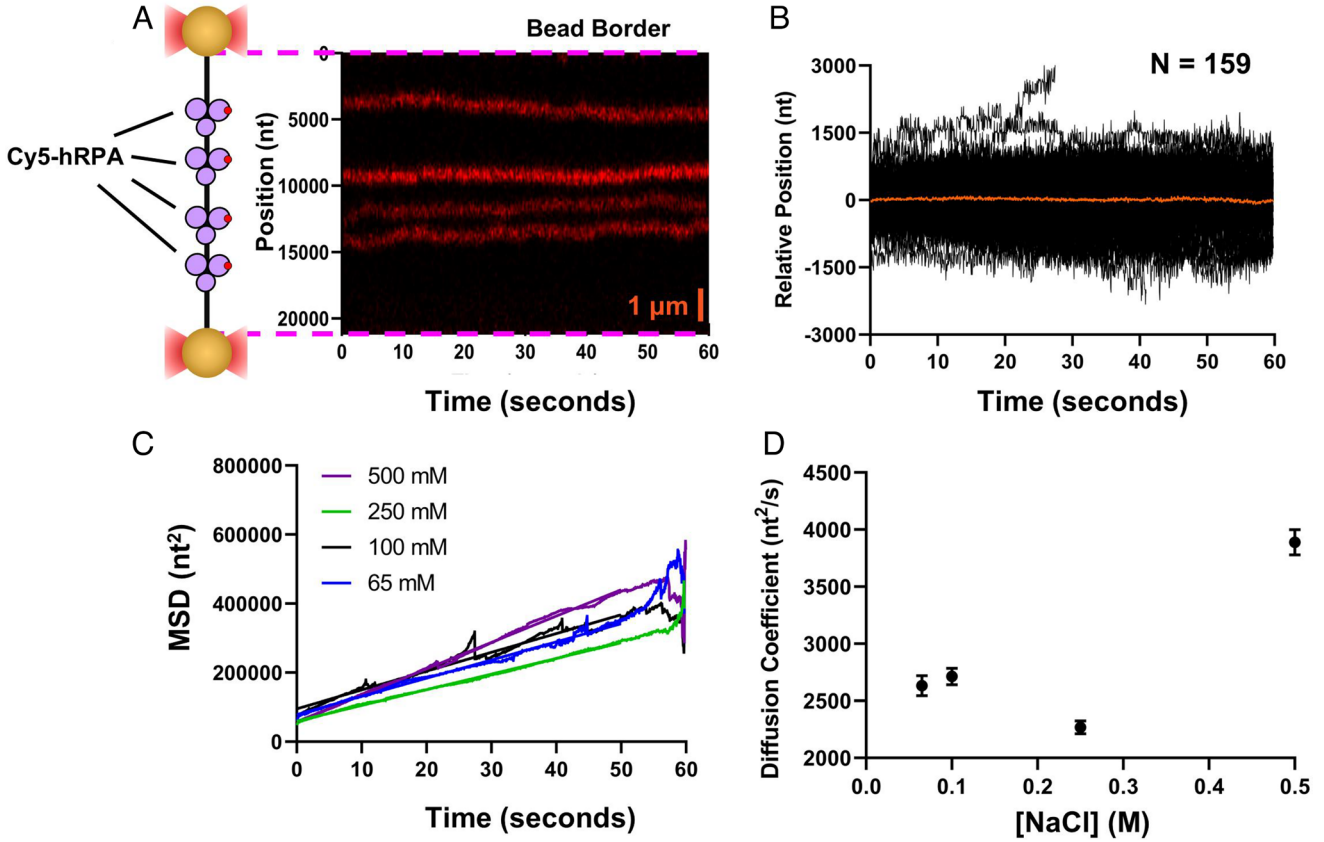

Fig. 2. Quantification of hRPA diffusion on single-stranded DNA. (*A*) Cy5-labeled hRPA was bound to ssDNA (20,452 nucleotides) that was immobilized between two streptavidin-coated polystyrene beads and held at constant force in a Lumicks C-Trap. Kymographs of four Cy5-hRPA molecules obtained by scanning the DNA length repetitively with a 638-nm excitation laser show the diffusive movements of Cy5-hRPA along the ssDNA. (*B*) Trajectories from 159 Cy5-RPA molecules are shown (each offset to begin at a position of zero) for ssDNA under 10 pN of tension. The orange line shows that the mean displacement for the entire dataset is zero indicating that Cy5-hRPA moves stochastically along ssDNA. (*C*) The mean squared displacement (MSD) of Cy5-hRPA on ssDNA held at 10 pN of tension at various [NaCl] was fit with linear lines to 50 s. (See Table 1 for diffusion coefficients). (*D*) The mean D_1 for Cy5-hRPA diffusion at 65 mM, 100 mM, 250 mM, 500 mM NaCl. Each data point is the mean D_1 ± 95% CI of the fit of the data in Fig. 2*C*.

shows the averaged MSD values as a function of time obtained at each [NaCl], and the values of D_1 at each [NaCl] are plotted in Fig. 2*D*. We find that D_1 is relatively constant at ~2,500 ± 200 nt^2/s between 65 mM and 250 mM NaCl, but increases to 3,888 ± 110 nt^2/s at 500 mM NaCl. The data at 500 mM NaCl allow us to compare these results from the Lumicks' experiments with our previous estimates of hRPA diffusion coefficient that were also made at 500 mM NaCl, but using only smTIRF microscopy. We find good agreement between the D_1 estimated from our previous smTIRF study (3) at 500 mM NaCl, interpolated to 30 °C (3,600 ± 300 nt^2/s) and the Lumicks' C-trap measurements under the same conditions (3,888 ± 110 nt^2/s).

ScPif1 Translocase Can Push Replication Protein A along ssDNA. We next investigated the behavior of hRPA in the presence of an ATP-dependent ssDNA translocase. We wanted to examine the effects of a heterologous translocase and RPA pair so that there would be no specific interactions between the two proteins; hence, we chose the *Saccharomyces cerevisiae* (Sc) Pif1 and the human RPA protein. We first performed smTIRF experiments to observe ScPif1 translocation and pushing of hRPA using the short $(dT)_{60}$ ssDNA (3'-dT-Cy3-$(dT)_{60}$) described above. Upon addition of unlabeled ScPif1 and ATP in buffer A, we observed the appearance of time trajectories showing rapid Cy3 fluorescence fluctuations (Fig. 3*A*). These Cy3 fluctuations result from repetitive ATP-dependent ScPif1 translocation events on ssDNA (12, 16). A Cy3 enhancement occurs when unlabeled ScPif1 encounters the Cy3 fluorophore at the 3′ end of the $(dT)_{60}$ due to protein-induced Cy3 fluorescence enhancement (PIFE) (17, 18). Because Pif1 preferentially binds to the ds/ssDNA junction, translocation of Pif1 to the 3′ end results in ssDNA looping (16). After reaching the 3′ end, Pif1 releases the 3′ end while remaining bound to the ss/ds DNA junction, thereby resulting in repetitive translocation cycles and repetitive Cy3 enhancements (16).

The same experiment was then performed by first adding Cy5-hRPA followed by unlabeled ScPif1 plus ATP. In this case, we observed a decrease in the number of time trajectories displaying the FRET signals associated with Cy5-RPA diffusion, and a concomitant increase in the Cy3 fluctuations associated with repetitive ScPif1 translocation. However, in the midst of these rapid Cy3 fluorescence fluctuations, we observe occasional isolated asymmetric Cy5 fluorescence increases and concomitant Cy3 fluorescence decreases resulting in a FRET spike (Fig. 3*B* and *SI Appendix*, Fig. S3 *B* and *C*). These events are similar to those observed in a previous study of *E. coli* SSB protein and ScPif1 (12). These asymmetric FRET spikes indicate that Cy5-hRPA is being chemomechanically pushed by the 5′ to 3′ translocase activity of ScPif1 toward the 3′ end and eventually displaced from it. No FRET spikes are observed in the absence of ATP. Furthermore, the time it takes for the signal to rise from the zero FRET baseline to the peak FRET signal decreases with increasing ATP concentration indicating a coupling of these events to the ScPif1 ATPase activity (*SI Appendix*, Fig. S3 *D* and *E*) (12, 19).

Table 1. Cy5-hRPA diffusion coefficients

Diffusion coefficient (nt^2/s), mean ± 95% CI	Force (pN), mean ± SD	# of videos	# of traces (N)	[NaCl] (M)
2,713 ± 72	10.0 ± 0.06	34	159	0.1
2,982 ± 55	7.5 ± 0.07	34	137	0.1
2,723 ± 55	5.1 ± 0.04	13	43	0.1
3,888 ± 110	10.0 ± 0.06	21	46	0.5
2,267 ± 87	10.0 ± 0.16	25	50	0.25
2,633 ± 87	10.13 ± 0.18	5	22	0.065

To quantitatively examine ScPif1 pushing of hRPA along ssDNA, we again utilized a Lumicks' C-Trap equipped with a scanning confocal laser to observe the movement of Cy5-hRPA along the 20,452 nucleotide ssDNA in the presence of ScPif1 and ATP (Fig. 4*A*). Experiments were performed by moving the ssDNA tether held under force (10 pN) with bound Cy5-hRPA in buffer B into a channel containing 100 nM ScPif1 and 5 mM ATP in buffer B at 30 °C (*SI Appendix*, Fig. S1*A*). Once moved into the channel containing ScPif1 and ATP, the Cy5-hRPA molecules showed unidirectional movement toward one end of the ssDNA (red kymographs in Fig. 4*A*). Since it is well established that ScPif1 is a 5′-to-3′ ssDNA translocase (16, 19), this indicates the orientation of the ssDNA. Each Cy5-hRPA was tracked until it reached the polystyrene bead or until the signal disappeared indicating either photobleaching or dissociation of hRPA. Each kymograph was fit by linear regression to obtain a pushing rate of 310 ± 76 nt/s (89 traces) at 5 mM ATP and 184 ± 77 nt/s (78 traces) at 0.5 mM ATP (buffer B, 100 mM NaCl, 30 °C) (Fig. 4*C*). The slower rate at 0.5 mM ATP indicates the directional movement of Cy5-hRPA is dependent on the ATPase activity of the ScPif1 translocase.

We also determined the translocation rate of ScPif1 by itself in the absence of pushing Cy5-hRPA by utilizing a ScPif1 variant containing an N-terminal 6x-His tag. The ScPif1 variant was labeled by binding it to an anti-6x-His Tag monoclonal antibody conjugated to a DyLight™ 550 Fluorophore (DyL550(IgG)). The DyL550(IgG)-ScPif1 was then bound to the ssDNA tether in buffer B before being moved to a channel containing buffer B plus 5 mM ATP (*SI Appendix*, Fig. S1*A*). A kymograph (green) showing the directional movement of the DyL550(IgG)-ScPif1 along the ssDNA is shown in Fig. 4*B*. The DyL550(IgG)-ScPif1 kymographs were analyzed by linear regression yielding a translocation rate of 312 ± 68 nt/s (26 traces) at 5 mM ATP (Fig. 4*C*). At this saturating ATP concentration, the rate of DyL550(IgG)-ScPif1 translocation alone is identical to the rate for ScPif1 translocation while pushing Cy5-RPA. However, we do observe that the rate of hRPA dissociation from ssDNA increases (~fivefold to sevenfold) during Pif1 pushing events (compare *SI Appendix*, Figs. S2 and S4) indicating some hRPA can be displaced from the DNA during the pushing events.

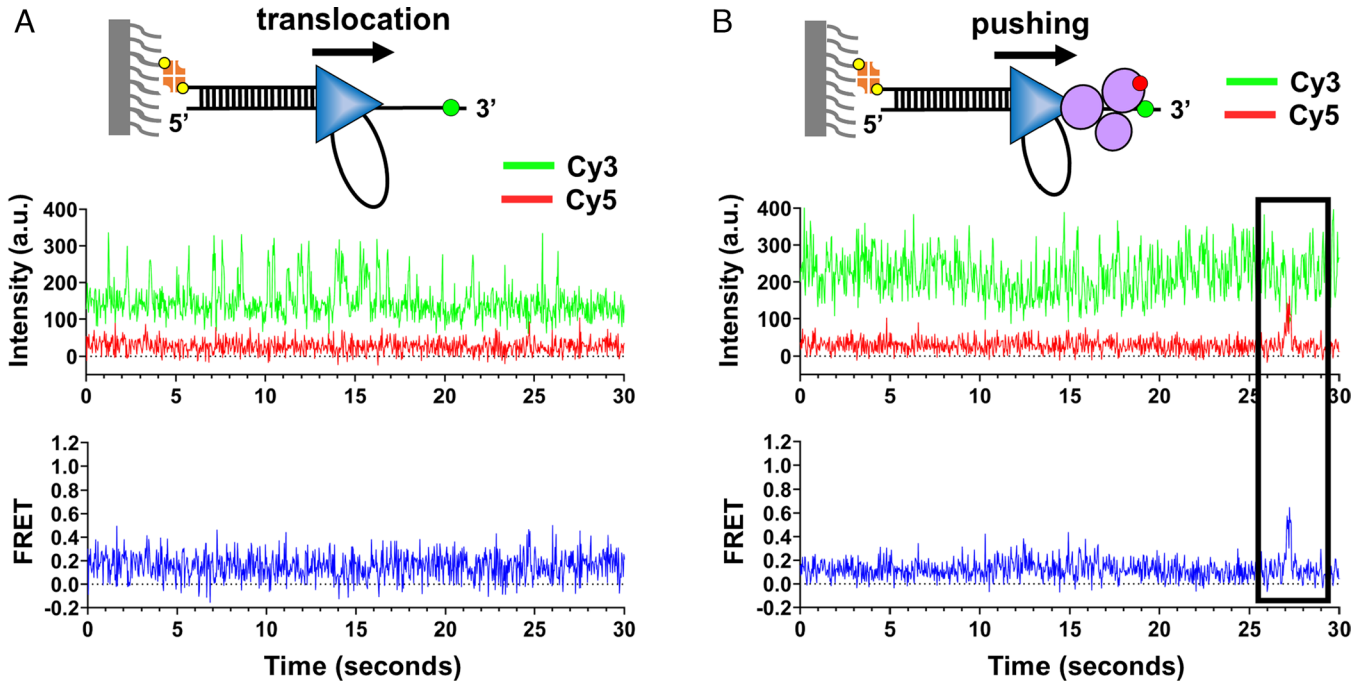

Fig. 3. Translocating Pif1 pushes hRPA off single-stranded DNA. (*A*) Representative time trajectory from a smTIRF experiment using a 3′ Cy3-labeled $(dT)_{60}$ ssDNA substrate immobilized on the surface of a coverslip in the presence of 100 nM Pif1 (schematically depicted in the cartoon as a blue triangle) and 5 mM ATP. Spikes of Cy3 fluorescence enhancement can be observed as Pif1 comes in close contact with Cy3 (331 out of 380 trajectories showed Cy3 spikes). (*B*) Before the addition of Pif1 and ATP, 100 pM Cy5-hRPA (shown in the cartoon as magenta circles) was added to the DNA, and unbound protein was removed by washing. The anticorrelated changes in the Cy3 and Cy5 time trajectories and the associated FRET spike (boxed in black) result from Cy5-hRPA being pushed off the end of the Cy3-labeled ssDNA by Pif1. Analysis of 1,573 trajectories showed 161 pushing events.

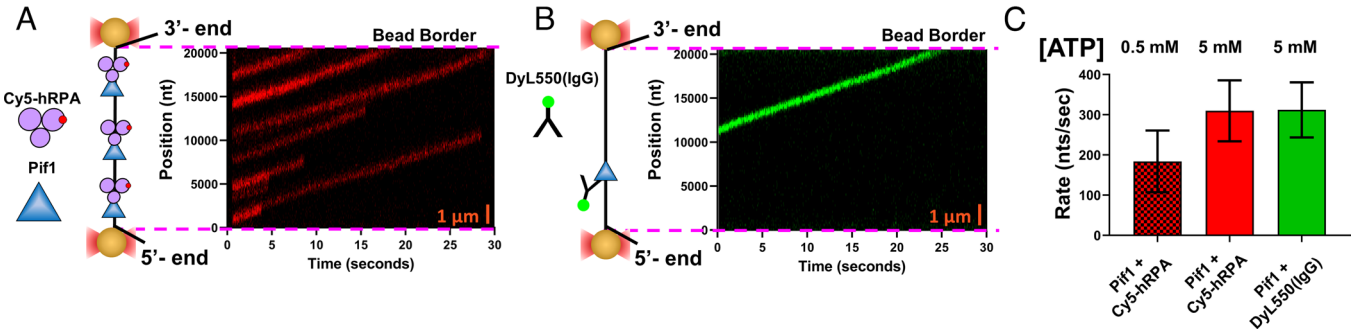

Fig. 4. Translocating Pif1 pushes hRPA along single-stranded DNA. (*A*) Cy5-hRPA was bound to a ssDNA tether as described in Fig. 2*A*, followed by incubation with 100 nM Pif1 and 5 mM ATP. Kymographs of several Cy5-hRPA molecules (scanning the length of the DNA repetitively with a 638-nm laser) show Pif1-dependent directional movement of Cy5-hRPA along the ssDNA (*B*) Translocation of Pif1 alone was monitored by binding DyL550(IgG)-labeled Pif1 to DNA in the same configuration as *A*, followed by incubation with 5 mM ATP. Kymograph of a representative DyL550(IgG)-Pif1 moving directionally along the ssDNA tether. (*C*) Average rates of the Pif1 pushing Cy5-hRPA in the presence of 5 mM ATP (red, 89 traces) or 0.5 mM ATP (red and black checker, 78 traces). The average translocation rate of DyL550(IgG)-labeled Pif1 alone was measured in the presence of 5 mM ATP (green, 26 traces).

ScPif1 Can Push hRPA into Duplex DNA Causing Stable Base Pair Disruption. Nguyen et al. (3) showed that hRPA is able to transiently disrupt a few bp of a duplex DNA hairpin by diffusing into the hairpin from an adjacent ssDNA loading site. However, the results indicated that the ability for hRPA to disrupt a hairpin is limited to less than ~9 bp of a 18-bp hairpin (3). Since we have shown here that ScPif1 can push hRPA along ssDNA, we investigated whether ScPif1 can apply a continuous force to hRPA that can cause a stable disruption of a DNA hairpin beyond the limit observed with hRPA alone.

To examine hairpin disruption, we designed a DNA containing a $(dT)_{45}$ -ssDNA region with an 18-bp hairpin at the 3′ end that contains a Cy3 label located in the middle of the hairpin duplex, 9 bp from both the loop and the ss/dsDNA junction (Fig. 5*A*). All smTIRF experiments were performed in buffer A with a 532-nm laser to excite Cy3 fluorescence. Again, we used a DNA substrate with a cyanine fluorophore incorporated into the DNA backbone via phosphoramidite linkages, which have minimal effect on the thermodynamic stability of duplex DNA (20, 21). Upon addition of 100 pM Cy5-hRPA to this surface-bound DNA and subsequently washing out unbound Cy5-hRPA, no changes in Cy3 or Cy5 signals are observed (Fig. 5*A*) indicating that Cy5-hRPA alone is unable to disrupt enough of the duplex DNA to reach the Cy3 fluorophore and elicit a FRET signal. However, upon addition of ScPif1 (100 pM) and 50 µM ATP to the Cy5-hRPA/DNA complex, we observe time trajectories with long-lived high FRET signals (Fig. 5 *B* and *C* and *SI Appendix*, Fig. S5) indicating that ScPif1 can push the Cy5-hRPA causing it to disrupt the duplex and reach the Cy3 fluorophore located 9 bp internally within the duplex DNA.

Long-lived FRET signals were observed in 194 out of 714 trajectories collected. The 194 trajectories yielded 231 FRET events, 111 of which began and ended within the timeframe of the trajectory with dwell times, Δt, as indicated in Fig. 5*C* and *SI Appendix*, Fig. S5. The distribution of FRET dwell times, Δt, is shown in Fig. 5*D*. The 120 FRET events that began or ended outside of the imaging timeframe were not included in the dwell time analysis. The loss of the FRET signal likely results from dissociation of either one or both of the proteins from the DNA. The distribution of FRET dwell times in Fig. 5*D* was fit to a sum of two exponentials, with observed rate constants, $k_1 = 0.33 \pm 0.25$ s^{-1} ($A_1 = 87$) and $k_2 = 0.04 \pm 0.02$ s^{-1} ($A_2 = 13$). These rates do not reflect the rate of Cy5 photobleaching, since the Cy5 fluorescence is stable for minutes under these conditions. The two rates of FRET loss may result from the fact that RPA can bind ssDNA in different modes that occlude different amounts of ssDNA (20 nt vs. 30 nt) (3, 22). These different RPA conformational states may result in different stabilities for hRPA on ssDNA while being pushed by ScPif1. It has also been observed that RPA dissociation from ssDNA occurs via a two-exponential decay (23), likely reflecting different rates of dissociation for these two binding modes. The existence of two phases may also result from a partitioning of the ScPif1 translocase between two conformational states, as found previously (19) in studies of ScPif1 monomer translocation along ssDNA. Interestingly, the rate constant for the slower rate of FRET loss is similar to the rate of hRPA dissociation while being pushed by Pif1 along ssDNA (*SI Appendix*, Fig. S4). Regardless, these data indicate that ScPif1 can push Cy5-hRPA into the duplex DNA to reach the Cy3 and that Cy5-hRPA remains near the Cy3 before either dissociating or returning to the ssDNA region.

As a control, we tested whether ScPif1 could unwind the 5′-ssDNA tailed hairpin DNA in the absence of Cy5-hRPA at the Pif1 and ATP concentrations at which Cy5-hRPA is pushed into the duplex DNA (*SI Appendix*, Fig. S6). In the absence of ScPif1, a stable Cy3 fluorescence signal is observed for DNA alone (*SI Appendix*, Fig. S6 *A* and *C*). Upon addition of high concentrations of ScPif1 (≥1 nM) and high [ATP] (5 mM), significant Cy3 fluorescence fluctuations (Cy3-PIFE signals) are observed indicating that ScPif1 can unwind the DNA and reach the Cy3 fluorophore (*SI Appendix*, Fig. S6 *B* and *C*). However, no such Cy3 PIFE signals were observed at a ScPif1 concentration of 100 pM and 50 µM ATP (*SI Appendix*, Fig. S6*C*), indicating that ScPif1 alone cannot unwind the DNA to reach the Cy3 at the concentrations used in the RPA pushing experiments. This is consistent with the observation that a monomer of ScPif1 cannot unwind a dsDNA with only a single 5′ flanking ssDNA (24, 25). Thus, the high-sustained FRET events observed in Fig. 5*B* with Cy5-hRPA and 100 pM ScPif1 and 50 µM ATP are due to Cy5-RPA being pushed into the duplex by the translocase activity of ScPif1, since at these conditions no DNA unwinding (helicase) activity is detected with ScPif1 alone.

The absence of a sharp Cy3 fluorescence increase before the steady rise in FRET indicates that ScPif1 is translocating behind and pushing Cy5-hRPA rather than ScPif1 first unwinding the DNA followed by hRPA binding to the newly generated ssDNA behind the ScPif1 helicase. In further support of this conclusion, when the ssDNA contains a 3′-3′ reverse polarity phosphodiester

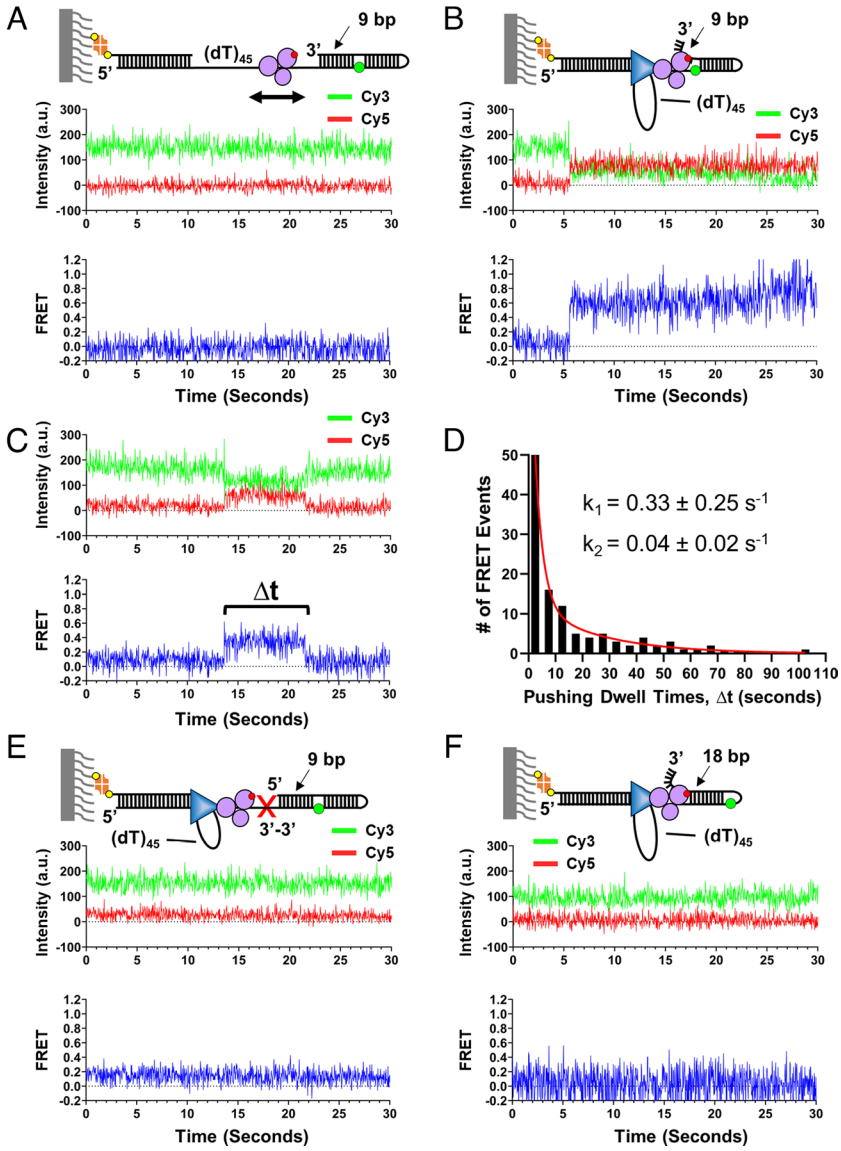

Fig. 5. Pif1 pushes Cy5-hRPA to stably disrupt a 9-bp duplex. (*A*) Cy5-hRPA was bound to a surface immobilized DNA with a $(dT)_{45}$ ssDNA region followed at the 3′ end by an 18-bp hairpin. As depicted in the cartoon, a Cy3 is placed in the backbone at 9 bp from the ss/dsDNA junction. No FRET events were observed after incubation with 100 pM of Cy5-hRPA, followed by removal of unbound Cy5-hRPA (770 trajectories). (*B* and *C*) After 100 pM Pif1 and 50 μM ATP were added to Cy5-hRPA/DNA complexes, high FRET signals appear that are either long lived as in *B* or with a clearly defined dwell time, Δt, as in panel *C*. These indicate that Cy5-hRPA has moved closer to the Cy3 fluorophore located in the center of the hairpin. FRET events were observed in ~27% of the single-molecule trajectories (194 out of 714 trajectories). 231 FRET events were observed in the 194 trajectories. (*D*) A histogram of dwell times (111) that initiated and ceased during imaging, as shown in 5*C* and *SI Appendix*Fig. S5. The data were fit to a sum of two exponentials, $Y = A_1 * e^{k_1 * t} + A_2 * e^{k_2 * t}$, with $A_1 = 87$ and $A_2 = 13$. (*E*) DNA substrate similar to that in panel (*A*), but with a reverse polarity linkage (red X) between the $(dT)_{45}$ linker and 18-bp hairpin. No FRET signals were observed in either the presence of Cy5-hRPA alone (582 trajectories) or Cy5-hRPA in the presence of 100 pM Pif1 and 5 mM ATP (984 trajectories). (*F*) When Cy3 was placed in the backbone at 18 bp from the ss/dsDNA junction (instead of 9 bp as in A-C) FRET events were not observed in either the presence of only Cy5-hRPA (189 trajectories) or the presence of only 100 pM Pif1 plus 50 μM ATP (285 trajectories).

linkage at the ss/dsDNA junction, no sustained high FRET signals are observed in the presence of bound Cy5-hRPA or with the addition of 100 pM ScPif1 and 5 mM ATP (Fig. 5*E*). This indicates that neither ScPif1 nor Cy5-hRPA can proceed past the reverse polarity linkage. Hence hRPA access to the hairpin is from the adjacent ssDNA. When these experiments were repeated using a DNA substrate in which the Cy3 was placed 18 bp from the ss/ds DNA junction (Cy3-18-bp hairpin), no FRET signals were observed in the presence of bound Cy5-hRPA and 100 pM ScPif1 and 50 μM ATP (Fig. 5*F*) or 5 mM ATP (*SI Appendix*, Fig. S7). Furthermore, FRET events were not observed in experiments with the Cy3-18-bp hairpin and bound Cy5-hRPA alone. Thus, the ability of ScPif1 to push Cy5-hRPA stably into the DNA duplex is limited to between 9 and 18 bp.

Discussion

The complementary single-molecule approaches used here show that hRPA protein is highly dynamic; it can diffuse along ssDNA and be pushed directionally by the ATPase activity of a ssDNA translocase, ScPif1. We also report direct estimates of the hRPA diffusion coefficient on ssDNA, the rate of ScPif1 translocation and the rate of ScPif1 pushing of hRPA along ssDNA using Lumicks' C-Trap. Finally, we demonstrate a mechanism for how hRPA, when combined with the heterologous ScPif1 (ATPase-driven) ssDNA translocase, can stably disrupt at least 9 bp of a duplex DNA as a result of hRPA being pushed directionally into the duplex DNA by the SF1 translocase. These results highlight the two basic mechanistic requirements needed for a processive

helicase. The helicase must have the ability to transiently destabilize the duplex DNA base pairs, and also the ability to use ATP to translocate directionally along the ssDNA. Here, we demonstrate that these two activities can be unlinked with base pair destabilization being supplied by the hRPA protein and directional translocation supplied by the Pif1 (ATPase-driven) translocase. This introduces opportunities to probe the basic mechanisms of helicases, and demonstrates the possibility that this "helicase" function could allow more flexibility in the regulatory control of genome expression at the levels of DNA repair and recombination.

Previous studies have shown that *E. coli* SSB proteins (6) and eukaryotic RPA proteins (3, 5) are able to diffuse along short ssDNA. Here, we observed the diffusive movements of hRPA directly on long ssDNA by tracking a fluorescently labeled hRPA along a ssDNA under tension in an optical trap. This approach enabled a direct estimate of the one-dimensional diffusion coefficient of hRPA on ssDNA. Diffusion measurements were performed with the ssDNA held at forces from 5 to 10 pN, tensions that are sufficient to destabilize DNA secondary structures that may be present at lower forces (26, 27). The measured diffusion coefficients show no dependence on force in this range. However, there is a significant increase in D_1 with increasing [NaCl], with D_1 ~3,888 ± 100 nt^2/s at 500 mM NaCl, ~2,800 ± 100 nt^2/s at 100 mM NaCl. Based on our previous estimates of D_1 for hRPA diffusion as a function of temperature (pH 8.1, 500 mM NaCl) using a smTIRF approach on short oligo(dT) DNA, we interpolate a value of D_1 = 3,600 ± 300 nt^2/s at 30 °C (3) in good agreement with our current estimate under identical solution conditions (500 mM NaCl).

Previous studies of *E. coli* SSB tetramer diffusion on ssDNA (6) estimated a much lower diffusion coefficient of ~300 nt^2/s (37 °C, pH 8.1, 500 mM NaCl, 10 mM $MgCl_2$) and concluded that SSB diffuses via a reptation mechanism in which the ssDNA forms local bulges that can then migrate via a random walk along the protein surface. It is likely that this mechanism also applies to RPA diffusion. A recent computational study of RPA diffusion on ssDNA concludes that a reptation mechanism is also most probable for RPA diffusion (28). We note that the RPA–ssDNA interaction involves some DNA bending (29), but not the extensive ssDNA wrapping that occurs in the fully wrapped SSB-ssDNA interaction in its $(SSB)_{65}$ binding mode (30). This difference likely contributes to the ~10-fold higher diffusion coefficient observed for RPA.

Several studies have examined the salt dependence of protein diffusion on duplex DNA (31–35). These conclude that a salt independent D_1 suggests a sliding mechanism in which the protein maintains continuous contact with the DNA. However, a D_1 that increases with salt concentration suggests a hopping contribution to diffusion, in which a local dissociation is followed by rapid rebinding. This follows from the fact that the dissociation rate constant for most protein–DNA interactions, including RPA, increases with increasing [NaCl] (36). Our observation that the diffusion coefficient of hRPA on ssDNA is relatively constant below 250 mM NaCl is consistent with a sliding (reptation) mechanism in this [NaCl] range. The increase in D_1 at the higher [NaCl] of 500 mM suggests that hRPA diffusion may involve a combination of sliding and hopping along the ssDNA in this range where hRPA-DNA binding is weaker. One caveat to consider is that the occluded binding site-size of RPA also decreases at [NaCl] below 100 mM (3, 22); hence, the decrease in protein-ssDNA contacts at lower [NaCl] may also influence D_1.

We further showed that ScPif1 is able to use its ATP-dependent unidirectional translocation activity to push hRPA along ssDNA held at 10 pN force at a rate of 310 ± 76 nt/s (5 mM ATP). We also find that ScPif1 on its own translocates on the ssDNA tether at the same rate as when it is pushing hRPA. Two limiting models have been proposed for how a translocating enzyme might push a diffusing protein directionally along ssDNA, a "direct pushing" model and a "moving barrier rectification" model (12). In the "direct pushing" model, a collision between ScPif1 and hRPA is perfectly inelastic, resulting in ScPif1 and hRPA moving as a single unit along ssDNA with the same velocity as ScPif1 alone (no load or friction from RPA). In the "moving barrier rectification" model, a Pif1 collision with RPA blocks the 5′ to 3′ translocation of Pif1 and also prevents RPA from taking a diffusive step in the 5′ direction; as a result, ScPif1 can only translocate toward the 3′ end of the ssDNA when RPA takes a diffusive step in the 3′ direction. In the moving barrier rectification model, the pushing rate would be considerably slower than the rate of translocation alone. If diffusion were the limiting factor, it would take >20 h for the RPA to move the length of the ssDNA used in our experiments. Therefore, the direct pushing model provides a better description of ScPif1 pushing of hRPA since the load from pushing hRPA has no effect on the Pif1 translocation rate (12).

Since we have measured both the diffusion coefficient of hRPA on ssDNA, D_1, and the rate of pushing of hRPA by Pif1, v, we can calculate the minimum force that Pif1 would need to apply on hRPA in order to maintain its translocation velocity. This is given by Force = k_BTv/D_1 (37), where k_B is Boltzmann's constant and T is absolute temperature. Using the following values (assuming 4 Å/nt for ssDNA): v = 300 nt/s = 1.2×10^{-7} m/s; T= 303 °K; D = 3,000 nt^2/s = 4.8×10^{-16} m^2/s, we estimate the minimum force applied by Pif1 to be 1.0 pN.

Finally, our studies reveal a mechanism for the stable disruption of a short region of duplex DNA that involves rectification by the Pif1 translocase of hRPA's ability to transiently disrupt a DNA duplex as depicted in Fig. 6. Under conditions where neither hRPA nor ScPif1 alone can disrupt the duplex region of an 18-bp hairpin, their combined actions instead stably open at least 9 bp of duplex to produce a 3′ ssDNA flanking region. Biologically, this type of activity may help with the resolution of DNA secondary structures that impair replication, recombination, and repair at sites of genomic maintenance. In this regard, we note that one function of Pif1 helicases is to remove obstacles that would otherwise impede efficient progression of DNA replication. For example, Pif1 stimulates DNA replication by unwinding stable G-quadruplexes (7, 38–40), removing proteins tightly bound to DNA (41, 42) or a Cas9-dependent R-loop (43). In these cases, the helicase activity of Pif1 appears to be needed to unwind the DNA in front of a DNA polymerase. However, here we show that the ssDNA translocase activity of Pif1 can also be used to destabilize a duplex DNA, by forcing an SSB protein into the duplex. Previous studies show that a single hRPA heterotrimer cannot transiently destabilize 9 bp of an 18-bp DNA hairpin (3), whereas here we show that ScPif1 can push a single hRPA into a hairpin, disrupting at least 9 bp for times that can exceed 1 min. The question remains, as to how the transient destabilization of a short duplex by RPA (3) or as shown here, the stable Pif1-dependent disruption of a longer duplex by RPA could be functional. Transient or stable opening of a short stretch of duplex DNA by these means may facilitate DNA repair processes that require the generation of a flanking 3′ ssDNA that could be used as a loading site for other proteins, such as RecA or RAD51 recombinases (44–48). Alternatively, since the 3′ end of a ss/ds junction of the duplex is a loading site for a DNA polymerase, its transient disruption by an SSB or stable opening by an SSB being pushed by a translocase could provide a means to regulate its use as a site for DNA synthesis.

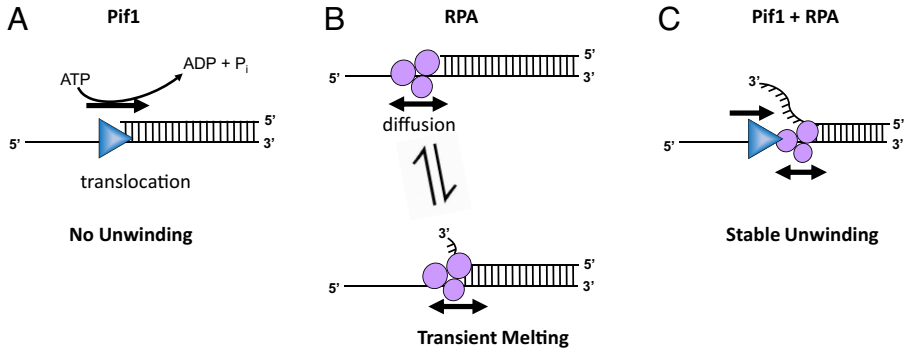

Fig. 6. RPA diffusion rectified by Pif1 translocation leads to stable DNA unwinding. (*A*) A Pif1 monomer can translocate along ssDNA, but it does not exhibit helicase activity on a single-tailed dsDNA. (*B*) RPA diffuses along ssDNA and can transiently melt a short region of duplex DNA. (*C*) When combined, the Pif1 translocase can rectify the transient DNA melting by RPA to stably unwind at least 9 bp of duplex DNA by applying a directional force to RPA at the junction.

We can only speculate as to why the RPA-Pif1 combined activity does not proceed further into the duplex beyond 9 to 18 bp. One possibility is that DNA duplex fluctuations within the partially unwound DNA may decrease compared to those at a ss/dsDNA junction. It also may be a consequence of the reptation mechanism that is likely used for RPA diffusion. As the RPA moves further into the duplex region, the formation of a transient bulge in the ssDNA may become more difficult, thus limiting further movement of RPA into the duplex. In addition, full-length RPA can bind polymeric ssDNA in multiple modes that differ in site size. In fact, a salt-dependent transition of the binding site size on poly(dT) has been reported for both yeast and human RPA from 20 to 22 nt to 28 to 30 nt (3, 22). RPA is composed of several OB-folds that all have the potential to bind ssDNA. The largest subunit, RPA70, contains 4 OB-folds (F-A-B-C). RPA32 contains one OB-fold (D) and RPA14 contains one OB-fold (E). The highest affinity OB-folds are the A and B OB-folds within RPA70. It has been estimated that the A and B OB-folds have a binding site size of ~8 to 9 nucleotides (29). Hence, it is possible that the limit of 9 to 18 bp may be due to a transition of the hRPA from its 30 nucleotide-binding site size to a smaller site size between 9 and 20 nucleotides when hRPA is pushed by Pif1 into the DNA duplex. These lower site size binding modes may have less ability to transiently invade further into the duplex.

We purposely used a heterologous translocase and RPA (SSB) pair from different organisms so that we could examine how RPA responds to the force exerted by a directionally translocating enzyme in the absence of any specific protein–protein interactions. The results in this study expand those obtained in a previous study of translocases pushing a tetrameric bacterial SSB protein (12). That study showed monomers of the superfamily 1 (SF1) ssDNA translocases, *E. coli* UvrD, *E. coli* Rep, and ScPif1, can directionally push *E. coli* SSB tetramers along ssDNA in reactions that are coupled to ATP hydrolysis (12). Rep and UvrD pushed SSB in the 3′ to 5′ direction, whereas Pif1 pushed SSB in the 5′ to 3′ direction, based on their known ssDNA translocase directionalities. That study also concluded that a "direct pushing" model provided a good description of the pushing of *E. coli* SSB protein along ssDNA by those translocases (12). There are numerous examples of SSB proteins from both prokaryotes and eukaryotes that can form specific interactions with a cognate ssDNA translocase (45, 49, 50). It will be of interest to examine how those interactions might influence the translocase rates and activity and also the ability of the SSB to invade a DNA duplex. While it remains possible that a homologous Pif1/RPA pair could potentially result in better "coupling" of ssDNA translocation with DNA opening, our use of a heterologous system demonstrates the generality of the observed behavior and the basic requirements to achieve "helicase" activity.

The results presented here also bear generally on the basic mechanistic requirements for processive helicases. It is now recognized that DNA unwinding (helicase) activity generally requires more than just ssDNA translocase activity (51). For example, the SF1 enzymes, Rep, UvrD, PcrA and *M. tuberculosis* UvrD1 monomers are rapid and processive ssDNA translocases, but have no detectable helicase activity by themselves (52–59). These enzymes require activation in order to function as helicases to unwind DNA. This can occur by dimerization (59, 60), removal of an autoinhibitory subdomain (52), or through an interaction with an accessory protein, PriC for Rep (61), MutL for UvrD (62, 63), and RepD for PcrA (64). Here we demonstrate a mechanism for how the combined action of a directional ssDNA translocase and a heterologous SSB protein can result in limited DNA unwinding activity. These two proteins provide the two basic activities needed for a processive helicase. The RPA heterotrimer provides the ability to transiently destabilize a short region of a DNA duplex (3). The presence of the chemomechanical translocase is needed to provide a directional force preventing (rectifying) the RPA from exiting the DNA duplex. This demonstrates the basic properties of a "helicase". One component (RPA) must destabilize the duplex DNA, while another component (ATP-dependent translocase) provides the force to prevent reformation of the duplex DNA. Furthermore, it reinforces the idea that the ATPase activity of a helicase is not generally needed to catalyze DNA base pair melting. DNA base pair melting can be accomplished due to the binding free energy of the SSB protein. The ATPase activity is needed solely to supply the directional translocation component. There is good evidence that this is the case for the RecBCD helicase (65).

Our study examined the consequences of a ssDNA translocase pushing and eventually displacing a single RPA heterotrimeric protein. It will also be of interest to examine whether a ssDNA translocase is able to push and displace multiple RPA proteins along ssDNA. Recent studies have shown that the human DNA helicase B (HelB) can use its 5′ to 3′ ssDNA translocase activity to displace multiple hRPA proteins from ssDNA (13). In that case, HelB appears to interact specifically with hRPA, and this interaction stimulates the translocase activity of HelB. No stimulation was observed with the heterologous yeast RPA. In fact, multiple yeast RPA proteins appeared to prevent HelB translocation along ssDNA. Although no evidence was presented concerning whether HelB can push the hRPA in those studies, it

seems likely that RPA pushing would precede RPA displacement.

Materials and Methods

Buffers. Buffer A is 30 mM TRIS (pH 8.1), 100 mM NaCl, 5 mM $MgCl_2$, 0.1 mM Na_2EDTA, 1 mM dithiothreitol, 0.5% (w/v) dextrose, 0.1 mg/mL bovine serum albumin, 4 mM 6-Hydroxy-2,5,7,8-tetramethylchroman-2-carboxylic acid (Trolox). Buffer B is 30 mM TRIS (pH 8.1), 100 mM NaCl, 5 mM $MgCl_2$, 0.1 mM Na_2EDTA, 1 mM dithiothreitol, 0.5% (w/v) dextrose, 4 mM 6-Hydroxy-2,5,7,8-tetramethylchroman-2-carboxylic acid (Trolox). PBS buffer is 137 mM NaCl, 2.7 mM KCl, 1.19 mM Phosphates, 500 μM EDTA and 5 mM NaN_3. Buffer X is 10 mM TRIS (pH 8.1), 50 mM NaCl, and 0.1 mM Na_2EDTA.

Oligodeoxynucleotide Synthesis. Oligodeoxynucleotides were synthesized on a MerMade 4 synthesizer (Bioautomation) using phosphoramidites (Glen Research). DNA purification and concentration were performed as previously described (3). DNA duplexes were annealed in buffer X as previously described (3). The sequences and structures of the oligodeoxynucleotides used in this study are shown in *SI Appendix*, Tables S1 and S2.

Protein Purification and Labeling. Human RPA (hRPA), *S. cerevisiae* Pif1, and *S. cerevisiae* Pif1 N-His were purified, and concentrations were determined by absorbance as previously described (3, 24, 66). hRPA was labeled stochastically as described (3) with Cy5 mono NHS ester (PA15101, Amersham, Piscataway, NJ) under conditions where the N-terminal amines are preferentially labeled. Labeling percentage as measured by UV-VIS absorbance was 92% (dye to hRPA ratio), indicating that while the hRPA was labeled stochastically among the three N termini, there was only one Cy5 per hRPA. Labeling occurred on 46% of Rpa1, 34.5% of Rpa2, and 11.5% of Rpa3 according to SDS–PAGE. Labeling percentage of the Cy5-hRPA used in the optical tweezers experiments was 148% (dye to hRPA ratio). The ScPif1-N-His protein was labeled by binding to a 6x-His Tag monoclonal antibody (500 nM) conjugated to a DyLight™ 550 Fluorophore (Cat. # MA1-21315-D550**,** ThermoFisher Scientific).

Single-Molecule Total Internal Reflection Fluorescence Microscopy (smTIRFM). smTIRFM experiments were conducted on an objective-based total internal reflection fluorescence microscope custom built from an IX71 inverted microscope (Olympus) with an 60× 1.45 numerical aperture PlanApo objective (Olympus) as described (3, 12). Briefly, biotinylated DNA substrates containing Cy3 were immobilized onto a polyethylene glycol (PEG, MW 5000)-coated coverslip via Neutravidin linkage to biotinylated PEG. The immobilized Cy3 substrates were excited by illumination from a 532-nm diode-pumped solid state laser (CrystaLaser, Reno, NV) coupled to the microscope using KineFlex fiber optics (QiOptics). All experiments were done at 25 °C using a temperature controlled stage (BC-110 Bionomic controller, 20/20 Technology Inc) and an objective heater (Bioptechs Inc.). Fluorescence emission was detected with an Andor iXon EMCCD camera (Model DU897E) and SINGLE, a custom program provided by Taekjip Ha (Johns Hopkins University), was used for movie collection. Movies were processed using custom scripts in IDL (Exelis VIS) to extract individual intensity vs time trajectories and then analyzed with MatLab (Mathworks). smTIRFM experiments were performed in buffer A and ATP concentrations as indicated for each experiment. An oxygen scavenging system [glucose oxidase (1 mg/mL final concentration) and catalase (0.4 mg/mL final concentration)] was added to all samples immediately before loading onto the TIRF slide.

Combined Optical Tweezer and Confocal Scanning. Diffusion of Cy5-hRPA, ATP-dependent translocation of ScPif1 and pushing of hRPA by ScPif1 was performed with a Lumicks' C-Trap controlled with Bluelake™ (v2.0) software. The combined optical tweezer and confocal scanning microscope is outfitted with a μ-Flux™ Microfluidics System (Lumicks) with a flow cell containing 5 channels (C1, Lumicks). The Lumicks C-Trap flow cell was passivated prior to performing experiments by flowing PBS (0.5 mL at 1.6 bar) through the syringes, lines, and flow cell, followed by flowing 0.5% (w/v) pluronic acid (0.5 mL at 1.6 bar, SKU00003, Lumicks and Pluronic® F-127 P2443, Sigma) and then 0.1% (w/v) BSA (0.5 mL at 1.6 bar, SKU00003, Lumicks and A-6793, Sigma). The passivation procedure is ended by flowing PBS (0.5 mL at 1.6 bar) through the same system. Please refer to *SI Appendix*, Fig. S1 to aid in the description below. Experiments begin by procuring streptavidin-coated polystyrene beads (4.89 um, SKU00003, Lumicks and 4.34 um Cat No.:SVP-40-5, Spherotech Inc.), in channel 1, within each of the two optical trapping lasers (1,064 nm). The beads within the traps are moved to channel 2 to bind a single 20,452-bp biotinylated DNA (SKU00014, Lumicks) to both beads. The duplex DNA tether is moved to channel 3 where a force is applied to stretch the DNA until the unattached DNA strand dissociates yielding a 20,452-nucleotide long ssDNA tether assembly. ssDNA formation was performed in a 1/10th dilution of PBS (SKU00003, Lumicks) and was confirmed to be ssDNA through visual confirmation on the screen that no hysteresis occurred during DNA extensions. Force applied to the ssDNA tether was measured by Trap 2, while Trap 1 was moved to manipulate force on the DNA. Protein-DNA complexes were formed in channel 4, and then imaged in channel 5. Channel 4 contained Cy5-hRPA at a concentration of 100 pM. Refer to *SI Appendix*, Fig. S1 for details.

Experiments quantifying the diffusional movements of Cy5-hRPA on ssDNA were performed using a feedback loop that maintains a constant force on the ssDNA. The temperature was regulated at 30 °C by temperature controllers on both the objective and condenser of the microscope. Diffusion measurements were performed using buffer B. Glucose oxidase (0.5 mg/mL final concentration) and catalase (0.2 mg/mL final concentration) were added to the solution just before placing the mixed solutions into the microfluidics system. A freshly prepared solution was placed into the microfluidics system every 2 h of image acquisition. Kymographs were acquired using a 638-nm laser at 4% power, 27.2-ms scanning line time, and a pixel size of 100 nm. Tracking of Cy5-hRPA molecules, mean squared displacement (MSD) of hRPA, and single-molecule diffusion coefficients were calculated in Pylake (v0.12.1, Lumicks) using python scripts (v3.10.5) executed within Jupyter Notebooks. Individual molecule kymograph images were obtained by implementing the greedy tracking algorithm, which finds pixels with intensities above a threshold and subsequently refines an area of interest to determine its subpixel position before linking positions on the same trajectory together to follow the position of the molecule over time. To enable more robust tracking, the time along the kymograph image was binned by two.

The mean squared displacement of Cy5-hRPA for each trace was calculated using Equation (1).

$$MSD = \frac{1}{N-n}\sum_{i=1}^{N-n}(x_{i-n}-x_i)^2 \qquad [1]$$

where n = lag number, N = number of points within the tracked line, and x_i = trace position at time frame i. The diffusion coefficients from the mean MSD were calculated by fitting the mean data from zero to 50 s using linear regression. The slopes of those best-fit lines were divided by two to obtain the mean diffusion coefficient (MSD = 2Dt).

Tracking and imaging of molecules during the Pif1 translocation experiments were performed as described for the diffusion experiments. Solution conditions were identical to those of the diffusion experiments, except that ATP was added in the translocation experiments. The tracked lines from the kymographs exhibiting pushing or translocation were placed into GraphPad Prism and fit by linear regression to measure the translocation rate.

Data, Materials, and Software Availability. All data are included in the article and/or *SI Appendix*.

ACKNOWLEDGMENTS. We thank Thang Ho for synthesis and purification of the oligodeoxynucleotides. This work was supported by NIH Grants 5R35GM136632 (to T.M.L.) and 1R35GM139508 (to R.G.) and American Cancer Society Grant PF-15-040-01-DMC (to J.E.S). The Lumicks C-Trap G2 was purchased with support from NIH Instrumentation grant S10OD030315.

Author affiliations: [a]Department of Biochemistry and Molecular Biophysics, Washington University School of Medicine, St. Louis, MO 63110-1093; and [b]Department of Chemistry, Salisbury University, Salisbury, MD 21801

1. R. Chen, M. S. Wold, Replication protein A: Single-stranded DNA's first responder: dynamic DNA-interactions allow replication protein A to direct single-strand DNA intermediates into different pathways for synthesis or repair. *Bioessays* **36**, 1156–1161 (2014).
2. M. S. Wold, Replication protein A: A heterotrimeric, single-stranded DNA-binding protein required for eukaryotic DNA metabolism. *Annu. Rev. Biochem.* **66**, 61–92 (1997).
3. B. Nguyen *et al.*, Diffusion of human replication protein A along single-stranded DNA. *J. Mol. Biol.* **426**, 3246–3261 (2014).
4. N. Pokhrel *et al.*, Dynamics and selective remodeling of the DNA-binding domains of RPA. *Nat. Struct. Mol. Biol.* **26**, 129–136 (2019).
5. F. E. Kemmerich *et al.*, Force regulated dynamics of RPA on a DNA fork. *Nucleic Acids Res.* **44**, 5837–5848 (2016).
6. R. Roy, A. G. Kozlov, T. M. Lohman, T. Ha, SSB protein diffusion on single-stranded DNA stimulates RecA filament formation. *Nature* **461**, 1092–1097 (2009).
7. R. Zhou *et al.*, SSB functions as a sliding platform that migrates on DNA via reptation. *Cell* **146**, 222–232 (2011).
8. K. S. Lee *et al.*, Ultrafast redistribution of E. coli SSB along long single-stranded DNA via intersegment transfer. *J. Mol. Biol.* **426**, 2413–2421 (2014).
9. A. G. Kozlov, T. M. Lohman, Kinetic mechanism of direct transfer of Escherichia coli SSB tetramers between single-stranded DNA molecules. *Biochemistry* **41**, 11611–11627 (2002).
10. S. Kunzelmann, C. Morris, A. P. Chavda, J. F. Eccleston, M. R. Webb, Mechanism of interaction between single-stranded DNA binding protein and DNA. *Biochemistry* **49**, 843–852 (2010).
11. B. Gibb *et al.*, Concentration-dependent exchange of replication protein A on single-stranded DNA revealed by single-molecule imaging. *PLoS One* **9**, e87922. (2014).
12. J. E. Sokoloski, A. G. Kozlov, R. Galletto, T. M. Lohman, Chemo-mechanical pushing of proteins along single-stranded DNA. *Proc. Natl. Acad. Sci. U.S.A.* **113**, 6194–6199 (2016).
13. S. Hormeno *et al.*, Human HELB is a processive motor protein that catalyzes RPA clearance from single-stranded DNA. *Proc. Natl. Acad. Sci. U.S.A.* **119**, e2112376119 (2022).
14. E. Antony, T. M. Lohman, Dynamics of E. coli single stranded DNA binding (SSB) protein-DNA complexes. *Semin Cell. Dev. Biol.* **86**, 102–111 (2019).
15. S. Suksombat, R. Khafizov, A. G. Kozlov, T. M. Lohman, Y. R. Chemla, Structural dynamics of E. coli single-stranded DNA binding protein reveal DNA wrapping and unwrapping pathways. *Elife* **4** (2015).
16. R. Zhou, J. Zhang, M. L. Bochman, V. A. Zakian, T. Ha, Periodic DNA patrolling underlies diverse functions of Pif1 on R-loops and G-rich DNA. *Elife* **3**, e02190 (2014).
17. B. Nguyen, M. A. Ciuba, A. G. Kozlov, M. Levitus, T. M. Lohman, Protein environment and DNA orientation affect protein-induced Cy3 fluorescence enhancement. *Biophys. J.* **117**, 66–73 (2019).
18. H. Hwang, H. Kim, S. Myong, Protein induced fluorescence enhancement as a single molecule assay with short distance sensitivity. *Proc. Natl. Acad. Sci. U.S.A.* **108**, 7414–7418 (2011).
19. R. Galletto, E. J. Tomko, Translocation of Saccharomyces cerevisiae Pif1 helicase monomers on single-stranded DNA. *Nucleic Acids Res.* **41**, 4613–4627 (2013).
20. W. Lee, P. H. von Hippel, A. H. Marcus, Internally labeled Cy3/Cy5 DNA constructs show greatly enhanced photo-stability in single-molecule FRET experiments. *Nucleic Acids Res.* **42**, 5967–5977 (2014).
21. C. Phelps, W. Lee, D. Jose, P. H. von Hippel, A. H. Marcus, Single-molecule FRET and linear dichroism studies of DNA breathing and helicase binding at replication fork junctions. *Proc. Natl. Acad. Sci. U.S.A.* **110**, 17320–17325 (2013).
22. S. Kumaran, A. G. Kozlov, T. M. Lohman, Saccharomyces cerevisiae replication protein A binds to single-stranded DNA in multiple salt-dependent modes. *Biochemistry* **45**, 11958–11973 (2006).
23. R. Chen, S. Subramanyam, A. H. Elcock, M. Spies, M. S. Wold, Dynamic binding of replication protein a is required for DNA repair. *Nucleic Acids Res.* **44**, 5758–5772 (2016).
24. S. P. Singh, A. Soranno, M. A. Sparks, R. Galletto, Branched unwinding mechanism of the Pif1 family of DNA helicases. *Proc. Natl. Acad. Sci. U.S.A.* **116**, 24533–24541 (2019).
25. S. P. Singh, K. N. Koc, J. L. Stodola, R. Galletto, A monomer of Pif1 unwinds double-stranded DNA and it is regulated by the nature of the non-translocating strand at the 3′-end. *J. Mol. Biol.* **428**, 1053–1067 (2016).
26. M. N. Dessinges *et al.*, Stretching single stranded DNA, a model polyelectrolyte. *Phys. Rev. Lett.* **89**, 248102 (2002).
27. A. Bosco, J. Camunas-Soler, F. Ritort, Elastic properties and secondary structure formation of single-stranded DNA at monovalent and divalent salt conditions. *Nucleic Acids Res.* **42**, 2064–2074 (2014).
28. G. Mishra, L. S. Bigman, Y. Levy, ssDNA diffuses along replication protein A via a reptation mechanism. *Nucleic Acids Res.* **48**, 1701–1714 (2020).
29. J. Fan, N. P. Pavletich, Structure and conformational change of a replication protein A heterotrimer bound to ssDNA. *Genes Dev.* **26**, 2337–2347 (2012).
30. S. Raghunathan, C. S. Ricard, T. M. Lohman, G. Waksman, Crystal structure of the homo-tetrameric DNA binding domain of Escherichia coli single-stranded DNA-binding protein determined by multiwavelength x-ray diffraction on the selenomethionyl protein at 2.9-A resolution. *Proc. Natl. Acad. Sci. U.S.A.* **94**, 6652–6657 (1997).
31. S. C. Piatt, J. J. Loparo, A. C. Price, The role of noncognate sites in the 1D search mechanism of EcoRI. *Biophys. J.* **116**, 2367–2377 (2019).
32. P. C. Blainey, A. M. van Oijen, A. Banerjee, G. L. Verdine, X. S. Xie, A base-excision DNA-repair protein finds intrahelical lesion bases by fast sliding in contact with DNA. *Proc. Natl. Acad. Sci. U.S.A.* **103**, 5752–5757 (2006).
33. I. Bonnet *et al.*, Sliding and jumping of single EcoRV restriction enzymes on non-cognate DNA. *Nucleic Acids Res.* **36**, 4118–4127 (2008).
34. G. Komazin-Meredith, R. Mirchev, D. E. Golan, A. M. van Oijen, D. M. Coen, Hopping of a processivity factor on DNA revealed by single-molecule assays of diffusion. *Proc. Natl. Acad. Sci. U.S.A.* **105**, 10721–10726 (2008).
35. J. H. Kim, R. G. Larson, Single-molecule analysis of 1D diffusion and transcription elongation of T7 RNA polymerase along individual stretched DNA molecules. *Nucleic Acids Res.* **35**, 3848–3858 (2007).
36. T. M. Lohman, Kinetics of protein-nucleic acid interactions: use of salt effects to probe mechanisms of interaction. *CRC Crit Rev. Biochem.* **19**, 191–245 (1986).
37. M. E. Fisher, A. B. Kolomeisky, The force exerted by a molecular motor. *Proc. Natl. Acad. Sci. U.S.A.* **96**, 6597–6602 (1999).
38. M. A. Sparks, S. P. Singh, P. M. Burgers, R. Galletto, Complementary roles of Pif1 helicase and single stranded DNA binding proteins in stimulating DNA replication through G-quadruplexes. *Nucleic Acids Res.* **47**, 8595–8605 (2019).
39. W. C. Griffin, J. Gao, A. K. Byrd, S. Chib, K. D. Raney, A biochemical and biophysical model of G-quadruplex DNA recognition by positive coactivator of transcription 4. *J. Biol. Chem.* **292**, 9567–9582 (2017).
40. D. Dahan *et al.*, Pif1 is essential for efficient replisome progression through lagging strand G-quadruplex DNA secondary structures. *Nucleic Acids Res.* **46**, 11847–11857 (2018).
41. M. A. Sparks, P. M. Burgers, R. Galletto, Pif1, RPA, and FEN1 modulate the ability of DNA polymerase delta to overcome protein barriers during DNA synthesis. *J. Biol. Chem.* **295**, 15883–15891 (2020).
42. M. E. Douglas, J. F. X. Diffley, Budding yeast Rap1, but not telomeric DNA, is inhibitory for multiple stages of DNA replication in vitro. *Nucleic Acids Res* **49**, 5671–5683 (2021).
43. G. D. Schauer *et al.*, Replisome bypass of a protein-based R-loop block by Pif1. *Proc. Natl. Acad. Sci. U.S.A.* **117**, 30354–30361 (2020).
44. P. Baumann, S. C. West, The human Rad51 protein: Polarity of strand transfer and stimulation by hRP-A. *EMBO J.* **16**, 5198–5206 (1997).
45. S. Awate, R. M. Brosh Jr., Interactive roles of DNA helicases and translocases with the single-stranded DNA binding protein RPA in nucleic acid metabolism. *Int. J. Mol. Sci.* **18**, 1233 (2017).
46. M. M. Cox, Motoring along with the bacterial RecA protein. *Nat. Rev. Mol. Cell Biol.* **8**, 127–138 (2007).
47. S. L. Lusetti, M. M. Cox, The bacterial RecA protein and the recombinational DNA repair of stalled replication forks. *Annu. Rev. Biochem.* **71**, 71–100 (2002).
48. S. C. Kowalczykowski, D. A. Dixon, A. K. Eggleston, S. D. Lauder, W. M. Rehrauer, Biochemistry of homologous recombination in Escherichia coli. *Microbiol. Rev.* **58**, 401–465 (1994).
49. R. M. Brosh Jr., *et al.*, Functional and physical interaction between WRN helicase and human replication protein A. *J. Biol. Chem.* **274**, 18341–18350 (1999).
50. D. Bagchi *et al.*, Single molecule kinetics uncover roles for E. coli RecQ DNA helicase domains and interaction with SSB. *Nucleic Acids Res.* **46**, 8500–8515 (2018).
51. T. M. Lohman, E. J. Tomko, C. G. Wu, Non-hexameric DNA helicases and translocases: Mechanisms and regulation. *Nat. Rev. Mol. Cell Biol.* **9**, 391–401 (2008).
52. K. M. Brendza *et al.*, Autoinhibition of Escherichia coli Rep monomer helicase activity by its 2B subdomain. *Proc. Natl. Acad. Sci. U.S.A.* **102**, 10076–10081 (2005).
53. W. Cheng, J. Hsieh, K. M. Brendza, T. M. Lohman, E., coli Rep oligomers are required to initiate DNA unwinding in vitro. *J. Mol. Biol.* **310**, 327–350 (2001).
54. K. S. Lee, H. Balci, H. Jia, T. M. Lohman, T. Ha, Direct imaging of single UvrD helicase dynamics on long single-stranded DNA. *Nat. Commun.* **4**, 1878 (2013).
55. A. Niedziela-Majka, M. A. Chesnik, E. J. Tomko, T. M. Lohman, Bacillus stearothermophilus PcrA monomer is a single-stranded DNA translocase but not a processive helicase in vitro. *J. Biol. Chem.* **282**, 27076–27085 (2007).
56. N. K. Maluf, J. A. Ali, T. M. Lohman, Kinetic mechanism for formation of the active, dimeric UvrD helicase-DNA complex. *J. Biol. Chem.* **278**, 31930–31940 (2003).
57. N. K. Maluf, C. J. Fischer, T. M. Lohman, A Dimer of Escherichia coli UvrD is the active form of the helicase in vitro. *J. Mol. Biol.* **325**, 913–935 (2003).
58. C. J. Fischer, N. K. Maluf, T. M. Lohman, Mechanism of ATP-dependent translocation of E.coli UvrD monomers along single-stranded DNA. *J. Mol. Biol.* **344**, 1287–1309 (2004).
59. A. Chadda *et al.*, Mycobacterium tuberculosis DNA repair helicase UvrD1 is activated by redox-dependent dimerization via a 2B domain cysteine. *Proc. Natl. Acad. Sci. U.S.A.* **119** (2022).
60. B. Nguyen, Y. Ordabayev, J. E. Sokoloski, E. Weiland, T. M. Lohman, Large domain movements upon UvrD dimerization and helicase activation. *Proc. Natl. Acad. Sci. U.S.A.* **114**, 12178–12183 (2017).
61. B. Nguyen, M. K. Shinn, E. Weiland, T. M. Lohman, Regulation of E. coli Rep helicase activity by PriC. *J. Mol. Biol.* **433**, 167072 (2021).
62. Y. A. Ordabayev, B. Nguyen, A. G. Kozlov, H. Jia, T. M. Lohman, UvrD helicase activation by MutL involves rotation of its 2B subdomain. *Proc. Natl. Acad. Sci. U.S.A.* **116**, 16320–16325 (2019).
63. Y. A. Ordabayev, B. Nguyen, A. Niedziela-Majka, T. M. Lohman, Regulation of UvrD helicase activity by MutL. *J. Mol. Biol.* **430**, 4260–4274 (2018).
64. L. T. Chisty *et al.*, Monomeric PcrA helicase processively unwinds plasmid lengths of DNA in the presence of the initiator protein RepD. *Nucleic Acids Res* **41**, 5010–5023 (2013).
65. T. M. Lohman, N. T. Fazio, How does a helicase unwind DNA?insights from RecBCD helicase. *Bioessays* **40**, e1800009 (2018).
66. S. Barranco-Medina, R. Galletto, DNA binding induces dimerization of Saccharomyces cerevisiae Pif1. *Biochemistry* **49**, 8445–8454 (2010).